

Compact Short Range RF Motion Sensor for Improved Inertial Navigation

Chenming Zhou, James Downey, Daniel Stancil, and Tamal Mukherjee

Department of Electrical and Computer Engineering
Carnegie Mellon University
Pittsburgh, PA, USA 15213

Abstract: Zero velocity update (ZUPT) algorithms are often employed to improve the accuracy of a Micro-Electro-Mechanical Systems (MEMS) based inertial navigation system. A compact RF motion sensor is proposed to identify zero velocity periods required by a ZUPTing system. The proposed RF motion sensor measures the distance relative to the ground by measuring the phase shift of the reflected wave and detects zero velocity periods by monitoring the distance change. The impact of noise on the sensor performance has been investigated. A prototype RF motion sensor is constructed to demonstrate the concept and some latest experimental results are reported.

Keywords: Inertial navigation, ZUPT, positioning and velocity sensor, direct conversion.

Introduction

There has been a growing interest to develop small size, time stable, and accurate navigation sensors in GPS-denied or GPS-inhibited environments such as indoors, underground, or urban canyons. Inertial navigation that uses a combination of gyroscopes and accelerometers is perhaps the only technique that operates independently of external assets and without prior knowledge of the environment. However, a miniature Inertial Measurement Unit (IMU) equipped only with accelerometers and gyroscopes does not provide acceptable accuracy owing to accumulated integration errors. A technique known as Zero Velocity Update (ZUPT) has been applied to reduce the accumulated error [1]. While estimating ZUPTs from the IMU data itself provides some improvement, an independent means for directly determining the time interval over which the ZUPT can take place is preferred.

A compact RF motion sensor---Terrain Relative Velocity (TRV) sensor--- is proposed to improve the accuracy of a MEMS based pedestrian inertial navigation system. The proposed TRV sensor measures the distance relative to the ground by measuring the phase shift of the reflected wave from the ground. A Zero velocity period is detected if the distance change over that time period is less than a given threshold.

One of the design constraints of a TRV sensor is that it must be small enough to be embedded into a shoe. Low power consumption is also a desirable feature since it will be powered by battery. To demonstrate the concept, we have constructed a prototype sensor using connectorized

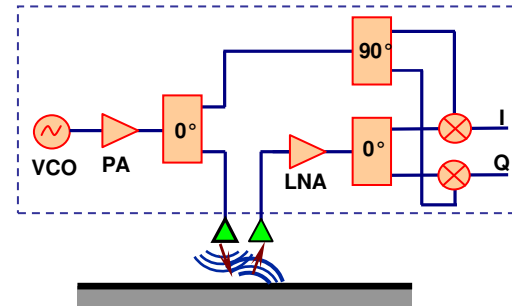


Figure 1. RF motion sensor: system block diagram

modular commercial off-the-shelf (COTS) components. Preliminary experimental results show that the TRV sensor can successfully detect zero velocity periods of a shoe during walking.

TRV Sensor: System Analysis

System Description: The system block diagram of the proposed TRV sensor is shown in Fig. 1. A single signal source provides both the RF output and LO signals, through a two way power splitter. The LO signal split from the source is further divided into two branches with a phase difference of 90-degree. These two orthogonal LO signals then mix with RF signals received by the receive antenna and output two intermediate frequency signals (here at zero frequency). A Power Amplifier (PA) and a Low Noise Amplifier (LNA) are added into the system to increase Signal to Noise Ratio (SNR). A direct conversion scheme has been employed considering the design constraints on power and size.

Let $\cos(\omega t)$ denote the single tone signal generated by the signal source, where ω is the angular frequency. The LO signal for the in-phase channel mixer can be represented as:

$$S_l(t) = A_l \cos(\omega t - \alpha_l), \quad (1)$$

where A_l and α_l are the amplitude and phase of the LO signal respectively. The RF signal before the mixer can be written as:

$$S_r(t) = A_r(d) \cos(\omega t - \alpha_r - \frac{4\pi fd}{c}), \quad (2)$$

where $A_r(d)$ is the amplitude of the RF signal, c is the speed of light, and α_r is a constant phase shift. Here d represents half of the path length that a signal travels when it is emitted from the transmit antenna, reflected by the ground, and finally detected by the receive antenna. The two antennas (RX and TX) are mounted on the same antenna plate with a separation distance of $2d_a$. Let \hat{d} denote the distance between the antenna plate and the ground plane, given by

$$\hat{d} = \sqrt{d^2 - d_a^2}. \quad (3)$$

The DC component output from the channel I/Q of the sensor is:

$$\begin{aligned} V_I &= A_s \cos(\theta_s) \\ V_Q &= A_s \sin(\theta_s) \end{aligned} \quad (4)$$

where $A_s(d) = \gamma \frac{A_t A_r(d)}{2}$, and $\theta_s(d) = \frac{4\pi f d}{c} - \alpha_0$. Here γ is the gain of the mixer and $\alpha_0 = \alpha_t - \alpha_r$.

Therefore, given measured voltages V_I and V_Q , an estimate of the path length d can be reconstructed from

$$d_{est} = \frac{c}{4\pi f} \left[\arctan\left(\frac{V_Q(d)}{V_I(d)}\right) + \alpha_0 + n\pi \right], \quad (5)$$

where d_{est} is the estimated path length and n is an integer to compensate for the phase ambiguity caused by the inverse tangent operation.

If the sensor always starts with a stance phase with a known initial path length d_0 , the unknown phase α_0 in (5) can be removed:

$$d_{est} = d_0 + \frac{c}{4\pi f} \left[\arctan\left(\frac{V_Q(d)}{V_I(d)}\right) - \arctan\left(\frac{V_Q(d_0)}{V_I(d_0)}\right) \right] \quad (6)$$

It should be noted that phase unwrapping should be considered in (6) if $d_{est} - d_0 > \lambda$. The velocity then can be obtained by differentiating the path length with respect to time

$$V_{est} = \frac{\Delta d_{est}}{\Delta t} \quad (7)$$

Noise Analysis: Eq. (6) assumes an ideal system where noise is absent. However, for a practical system, noise disturbances must be taken into account. In this section, we will investigate how noise presented in the system affects the distance and velocity reconstructions

The received noise-corrupted RF signal can be vectors, respectively. In the I/Q plane shown in Fig. 2, the single tone signal r_s is rotating with an amplitude of A_s and a

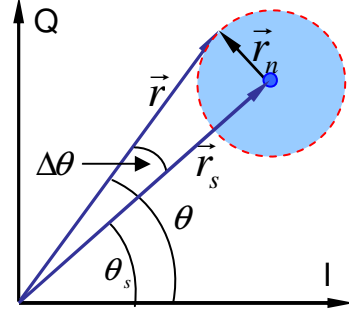


Figure 2. The impact of SNR on the distance reconstruction

constant angular velocity of ω , while the random noise vector is added onto the signal vector, with a phase θ_n equally random distributed in 360° over time, and a random amplitude A_n based on an appropriate probability distribution.

The presence of the noise vector causes the amplitude and phase of the corrupted signal to change randomly over time. Let $\vec{r} = A \angle \theta$, and $\Delta\theta = \theta - \theta_s$ denote the phase reconstruction error due to the noise disturbance. Given fixed A_n and signal vector \vec{r} , the phase estimation error $\Delta\theta$ is varying with θ_n . The noise vector \vec{r}_n is forming a circle in the I/Q plane as shown in Fig. 2 as θ_n is randomly changing. It is apparent that $\Delta\theta$ reaches its maximum value when \vec{r} is tangential to the circle of \vec{r}_n with a maximal value of

$$\Delta\theta_{max} = \arcsin\left(\frac{A_n}{A_s}\right). \quad (8)$$

Considering additive Gaussian noise with a zero mean and a standard deviation of σ , it is known that the possibility for $A_n \leq 2\sigma$ is 95.4%. Let $SNR = A_s^2 / 2\sigma^2$, the corresponding maximum distance estimation error (with 95.4% probability) is

$$\Delta d_{max} = \frac{c}{4\pi f} \cdot \arcsin\left(\sqrt{\frac{2}{SNR}}\right) \quad (9)$$

For high SNR, we have the approximation

$$\Delta d_{max} \approx \frac{c}{4\pi f} \cdot \sqrt{\frac{2}{SNR}} \quad (10)$$

According to (11), the system positioning accuracy is only dependent on two factors: operating frequency and system SNR. An increase of SNR and/or f results in better positioning accuracy.

Another application of (11) is to estimate the required minimum SNR to meet a target position resolution, assuming a noise limited system. e.g. for our system with

an operating frequency $f = 6.7$ GHz, to achieve a positioning resolution of 1 mm, the system SNR must be designed higher than 14 dB.

If the velocity is too low such that the distance of a sensor moved within two continuous samples separated by Δt is less than the above minimum distance error Δd_{max} , the system cannot give a reliable velocity estimation. Therefore, the position accuracy in (11) also sets a lower limit for the velocity that can be detected by the sensor. This minimum detectable velocity is simply determined by

$$V_{min} = \frac{\lambda}{4\pi \cdot \Delta t \cdot \sqrt{SNR/2}} \quad (11)$$

where $\lambda = c/f$ is the wavelength. For example, considering $f = 6.7$ Hz, $SNR = 20$ dB, and sampling rate of 10 Hz, a minimum detectable velocity of 5.04 mm/s can be obtained based on (11).

System Prototyping: To demonstrate the concept, a TRV sensor prototype has been built using COTS components, as shown in Fig. 3. The signal source is a Mini-Circuits (ZX95-6740C+) Voltage-Controlled Oscillator (VCO). A potentiometer is used to provide the necessary tuning voltage of the VCO. According to (11), a high system frequency is desirable since higher frequencies allow the design of smaller antennas and also provides better position resolution. The working frequency of 6.7 GHz is chosen in our prototype as a balance between the antenna size and commercially available components. The "mixers" module in Fig. 3 is a I/Q demodulation module including two mixers, one 90° power splitter, and one 0° power splitter. The "mixers" module is implemented with a single chip Hittite MMIC I/Q mixer module (HMC520LC4). All the components are mounted in a 8.7x6.3x2 inch aluminum box. Power consumption of the TRV prototype is about 1 Watt.

Performance Evaluation

System Stability Characterization: To evaluate the performance of the TRV sensor prototype, a stepper motor is used to accurately control the motion of the sensor. The position and velocity of the sensor can be computed based on the motion commands sent to the stepper motor, providing a "ground truth" reference for the performance of the sensor. The antenna plate is mounted on the carriage of the stepper motor. Two long (7 feet) RF cables are used to connect the Tx/Rx antennas with the TRV box. An op-amp is used to amplify the DC signals output from the TRV box. The data is sampled and collected by a National Instruments Data Acquisition (DAQ) system (NI-USB-6009) with a sampling rate of 100 samples/s. Both the DAQ and stepper motor are controlled by a laptop through Labview.

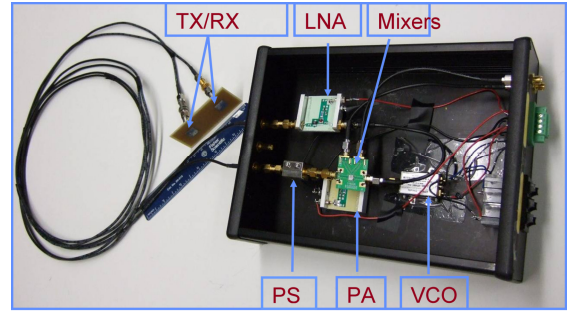


Figure 3. RF motion sensor based on COTS components

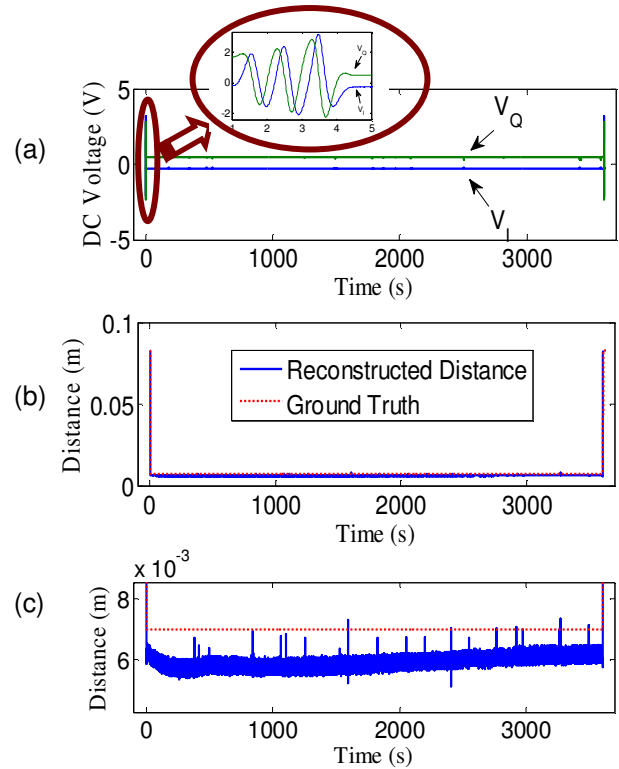


Figure 4. TRV sensor: Long term (one hour) position accuracy characterization. (a) shows the measured voltages $V_{I,Q}$ output from the sensor, (b) gives the reconstructed distance, and (c) is a zoomed in version of (b) in the Y axis.

A stability test was conducted to characterize the long term position accuracy of the proposed TRV sensor, especially when antennas are close to the reflectors where complicated interactions between antennas and the environment exist. For the stability test, the velocity of the stepper motor was set to 1 in/s and the acceleration was 0.2 in/s². The initial position of the sensor was measured as $d_0 = 0.083$ m and the antenna separation was $d_a = 0.02$

m. The motion of the stepper motor was programmed in the following way: 1) Stationary (1 s); 2) Constant velocity moving (forward) 3 inches; 3) Stationary (3600 s); 4) Constant velocity moving (backward) 3 inches; 5) Stationary (1 s).

The DC voltages collected from the I and Q channels over one hour are shown in Fig 4(a). The DC offsets in $V_{I,Q}$ have been removed by prior calibration. It is apparent that $V_{I,Q}$ vary with a sinusoidal pattern when the sensor is moving and are constant when the sensor is static. The reconstructed distance based on $V_{I,Q}$ is shown in Fig 4(b). The ground truth distance computed based on the motion commands sent to the stepper motor is also provided as a reference. As shown in Fig 4(b), the reconstructed distance curve agrees well with the computed ground truth. The maximum disagreement between the reconstructed position and the ground truth is about 1.5 mm. The major cause for this disagreement is the residual DC offset in the $V_{I,Q}$. It can be observed from Fig. 4(c) that distance drift caused by long time operation over one hour is less than 1 mm.

Walking Test: A preliminary walking in place test was conducted to demonstrate the functionality. Antennas are embedded in the heel of a boot as shown in Fig 5. Except antennas, the other components in Fig 5 are put on a table. Again, two RF cables are used to connect the antenna and the TRV box. For the experimental results reported here, the walking area was restricted by the limited length of the two cables and the motion of the foot is up and down only. The reflection interface is a typical flat concrete surface. The sampling rate for $V_{I,Q}$ acquisition is 10 k samples/s.

Fig 6 shows the experimental results for the first three steps of a total 100 steps. Fig 6(a) shows the collected DC voltages $V_{I,Q}$ during the walking. DC offsets in $V_{I,Q}$ have been removed. Fig 6(b) shows the reconstructed distance between the heel and the ground. It can be clearly observed from Fig 6(b) that the foot starts from a stationary phase with a zero distance and then experiences a motion phase where distance firstly increases and then decreases. The distance goes back to zero when the foot touches the ground and one step is accomplished. Zero velocity periods can be identified by monitoring the variation of the reconstructed distance. If the variance of the distance over a given time window is less than a chosen threshold, the TRV sensor reports a zero velocity period over that time window. The detected zero velocity periods are shown in Fig 6(c). In Fig 6(c), ZUPT=1/0 corresponds to zero velocity true/false.

Conclusions

A novel concept to use a compact RF motion sensor to improve the accuracy of pedestrian inertial navigation was

proposed and implemented. The preliminary experimental results show that the proposed TRV sensor can accurately sense its distance relative to the ground and detect zero velocity periods of a shoe during walking.

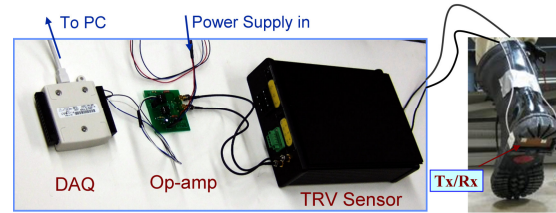


Figure 5. Experimental setup for walking tests.

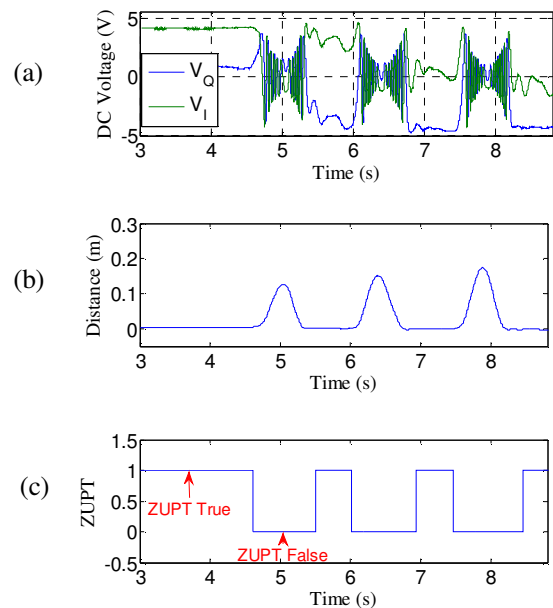


Figure 6. Experimental results of a walking test with a TRV sensor embedded into the heel. (a) shows the DC voltages output from the TRV sensor, (b) shows the reconstructed distance relative to the ground, and (c) gives the detected zero velocity periods of the shoe.

Acknowledgment¹

This material is based on research sponsored by the DARPA MINT Program under agreement number FA8650-08-1-7824.

References

1. E. Foxlin, "Pedestrian tracking with shoe-mounted inertial sensors," IEEE Comput. Graph. Appl., vol. 25, no. 6, pp. 38–46, Dec. 2005.

¹ Approved for Public Release, Distribution Unlimited

